ARTICLE | OPEN ACCESS

Indian journal of
Engineering

To Cite:
Hanafi AZ, Amer AH, Attia WA. Behavior of steel box girder bridges under blast loads and the possibility of reopening the bridge immediately following the explosion. *Indian Journal of Engineering*, 2024, 21, e10ije1685
doi: https://doi.org/10.54905/disssi.v21i55.e10ije1685

Author Affiliation:
[1]Department of Civil Engineering, Faculty of Engineering, Cairo University, Giza, Egypt
[2]Department of Civil Engineering, Elgazeera High Institute for Engineering, Cairo, Egypt

[*]**Corresponding Author**
Department of Civil Engineering, Faculty of Engineering, Cairo University, Giza,
Egypt
Email: ahmedhanifi2024@gmail.com

Peer-Review History
Received: 01 June 2024
Reviewed & Revised: 05/June/2024 to 05/August/2024
Accepted: 09 August 2024
Published: 12 August 2024

Peer-Review Model
External peer-review was done through double-blind method.

Indian Journal of Engineering
pISSN 2319–7757; eISSN 2319–7765

DISCOVERY
SCIENTIFIC SOCIETY

Behavior of steel box girder bridges under blast loads and the possibility of reopening the bridge immediately following the explosion

Ahmed Z Hanafi[1*], **Ahmed H Amer**[2], **Walid A Attia**[1]

ABSTRACT

Bridges play a vital role in transporting inhabitants and goods both within and outside of cities, making them vulnerable to explosions. Therefore, understanding how bridges perform under blast loads is crucial for the safety of infrastructure and urban societies. This research investigates the dynamic behavior of steel box girder bridges when exposed to blast loads, focusing on factors like explosive weight, blast standoff distance, and blast location. It also explores the possibility of partially reopening the bridge to traffic immediately after an explosion. We used the ABAQUS nonlinear finite element analysis software to model the bridge. The study shows that reinforced concrete slabs and steel girders completely collapse when subjected to an explosive weight of 5000 kilograms (equivalent to a truck filled with explosives). This indicates that these structural elements cannot withstand such a large explosion, leading to their total failure. Reinforced concrete slabs are more likely to collapse when an explosion occurs in the middle of the span, whereas steel box girders tend to collapse at the ends of a span. The detonation's standoff distance correlates with the explosive weight. Explosive weights of 50 kilograms (motorcycle) and 200 kilograms (medium car) damage specific areas of the bridge, allowing for the potential partial reopening of other sections immediately after the explosion. In contrast, explosive weights of 300 kilograms (large car), 1400 kilograms (pickup truck), and 3000 kilograms (van) cause extensive damage, making it impossible to reopen any section partially.

Keywords: Composite Bridges, Steel box girder, Blast loads, Explosive weight, Non-linear analysis

1. INTRODUCTION

With a rise in terrorist strikes and regional warfare, academics are becoming more concerned about the explosion danger of infrastructure. Bridges are essential for transporting people and goods both within and beyond cities. Because of their importance, they are especially vulnerable to explosions (Amer et al., 2020; Aamir et al., 2023; Lv et al., 2023). Terrorist terrorism has grown fast since the events of September 11, 2001, and its activities are now relatively common. Between 2002 and 2008, there were roughly 190 terrorist strikes on bridges worldwide (Stewart and Mueller, 2014). Explosions can occur because of both terrorist activities and vehicular crashes over bridges, emphasizing the importance of understanding explosion effects to prevent collapses. Many bridges are vital for trade and transportation and often serve as significant landmarks in their communities. Therefore, their destruction could have severe and far-reaching consequences. Therefore, it is critical to protect bridge structures against blast loads.

While significant research has explored the impact of blast loading on building structures and their components, studies on how bridges respond to blast loads remain limited. To safeguard infrastructure and urban environments, it is crucial to deepen our understanding of bridge behavior under such conditions. Researchers used simplified theory methods, such as Timoshenko beam theory and analysis of an equivalent single degree of freedom system, to study how concrete bridge structural components responded to blast loadings (Krauthammer et al., 1993; Low and Hao, 2002; Winget et al., 2005; Fujikura and Bruneau, 2011; Xiao et al., 2017; Anas and Alam, 2022). Although these simplified methods work well overall, they struggle to provide accurate estimates of localized effects. As computer technology and computational mechanics have advanced, researchers have increasingly used numerical simulations to study blast effects on structures. These simulations have proven effective in producing reliable predictions of structural responses (Zhou and Hao, 2008; Riedel et al., 2010).

In this study, we simulated the bridges using ABAQUS, (2017), a commercial finite element analysis tool. We applied the CONWEP model, available in ABAQUS for shock loading, to simulate the blast effects. This process involved creating an air blast scenario by applying an incident shock wave using the CONWEP model. This model calculates the shock wave's impact based on the explosive's TNT equivalence weight and the explosion's three-dimensional position. We computed the total pressure on the structural surface by considering incident pressure, reflected pressure, and the angle at which the blast wave hit the structure. This analysis is an empirical, uncoupled, dynamic analysis with multiple degrees of freedom. The CONWEP blast-loading model relies on traditional weapon effects calculations, uses several empirical equations, and curves (Hyde, 1988). One major advantage of the CONWEP model is that it calculates actual overpressure amplitudes (both positive and negative phases) and other blast wave properties based on a user-defined amount of TNT at a specific distance from the explosion source.

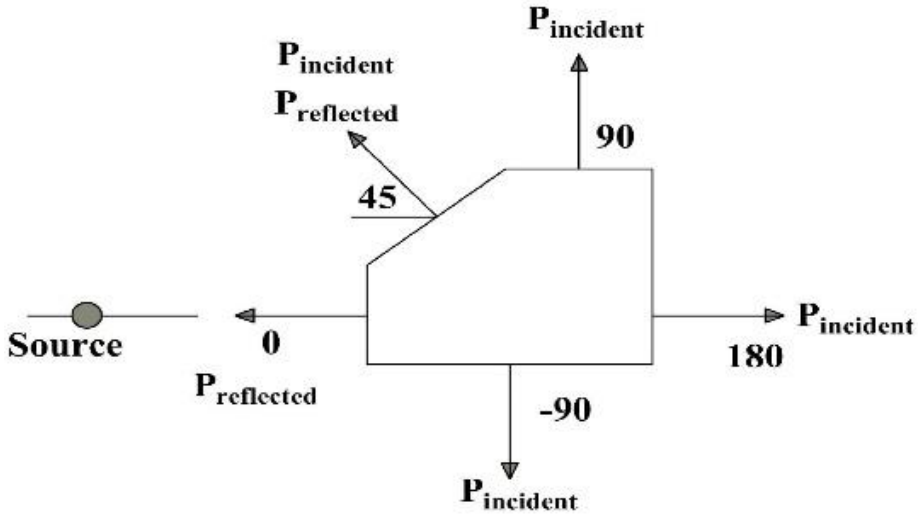

Figure 1 Blast wave reflection formulation adopted by CONWEP property

Additionally, the CONWEP model simplifies the process by not requiring the modeling of the fluid medium (such as air) to account for reflection effects. Figure 1 illustrates the reflection formulation that the CONWEP model uses. Composite steel box girder bridges have recently developed as a potential alternative to classic steel plate and concrete girder bridges. Many studies are investigating ways to enhance bridge design, durability, construction simplicity, and overall cost-effectiveness. Steel box girder bridges have intrinsic advantages over conventional plate girder bridges, including increased efficiency, less steel required for bending and shear due to their torsional rigidity, and improved live load distribution. Additionally, they reduce transverse bending in the deck, resulting in lower differential deflections (Lee et al., 2004; Braxtan et al., 2015; Vinitha et al., 2017). Figure 2 demonstrates how the torsional rigidity of a closed box girder section contributes to superior torsional behavior in bridges.

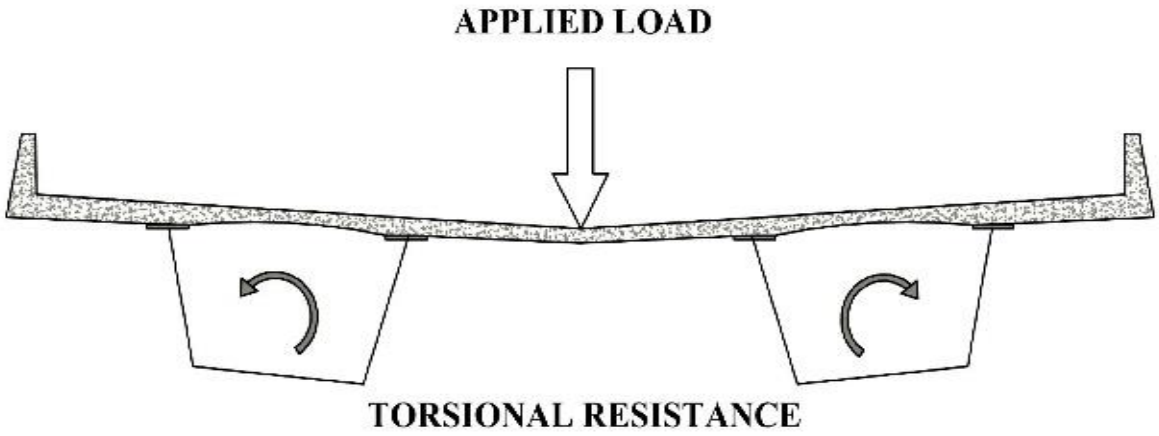

Figure 2 Live load distribution

However, there is little research on steel box girder cross-sections and their response to explosion events, which pose a significant risk to steel bridges. This research examined the dynamic behavior of steel box girder bridges exposed to blast loads and investigated relevant parameters, such as explosive weight, blast standoff distance, and blast location. The study also explored the possibility of partially reopening the bridge for traffic immediately after an explosion. The findings provide valuable insights into how similar bridges respond to various blast loads, helping engineers choose the most effective retrofitting methods to improve resistance to explosive effects.

Background

Nature of explosion

An explosion happens when energy suddenly releases into the atmosphere, creating a blast wave that expands outward from the source. This wave immediately boosts the ambient pressure to maximum overpressure, and its effect fades with time. Figure 3 depicts changes in overpressure as the distance from the explosion increases.

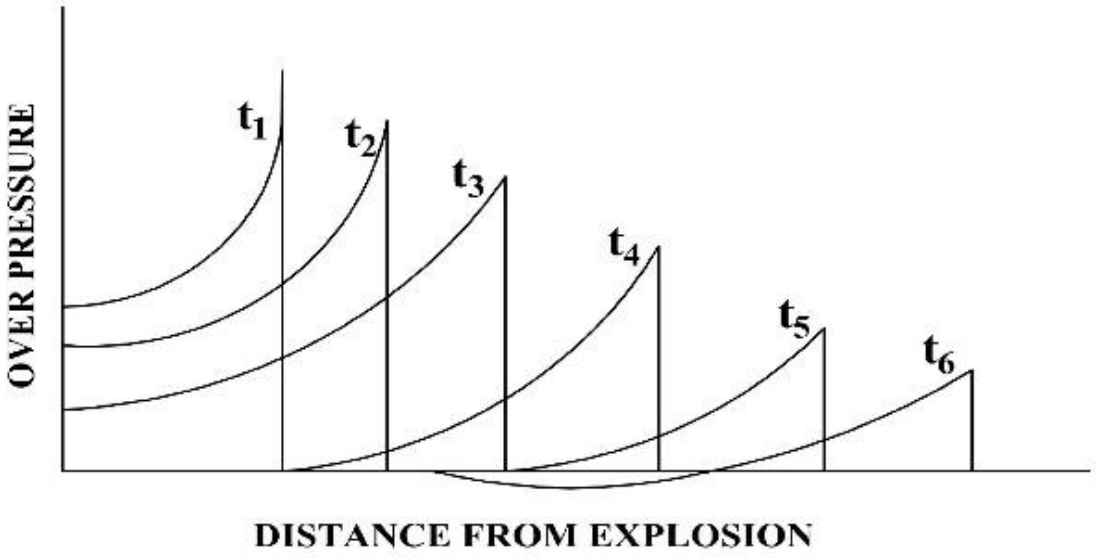

Figure 3 Overpressure variation with distance from explosion at successive time

There are three explosions: physical, chemical, and nuclear (Grys and Trzciński, 2010). Chemical explosions are the most prevalent kind of explosive that might occur accidentally or because of terrorist activities. The primary cause of a chemical explosion is the rapid oxidation of fuel ingredients, which might be liquids or solidified solids. Table 1 shows the values of explosive weights for various vehicles based on their carrying capacity (Xiao et al., 2017).

Table 1 The explosive weight of different vehicles

Carrier	Explosive weight (Kg)
Motorcycle	50
Medium Car	200
Large Car	300
Pick-up truck	1400
Van	3000
Truck	5000

Characteristics of blast wave

Blast characteristics create a rapid pressure pulse that spreads from the explosion. When an incident blast wave encounters a structure, it reflects, and the reflected pressure usually exceeds the incident pressure, depending on the angle of incidence. We calculate the reflected pressure value by multiplying the incident wave by the appropriate reflected pressure coefficient, as shown in (Figure 4). The blast pressure time history divides primarily into positive and negative phases. The positive phase typically causes more damage and can significantly harm the structure. The negative phase, which lasts longer and has a smaller impact, often, gets overlooked (TM 5-1300, 1990; Winget et al., 2005; Pan et al., 2013; Ullah et al., 2017).

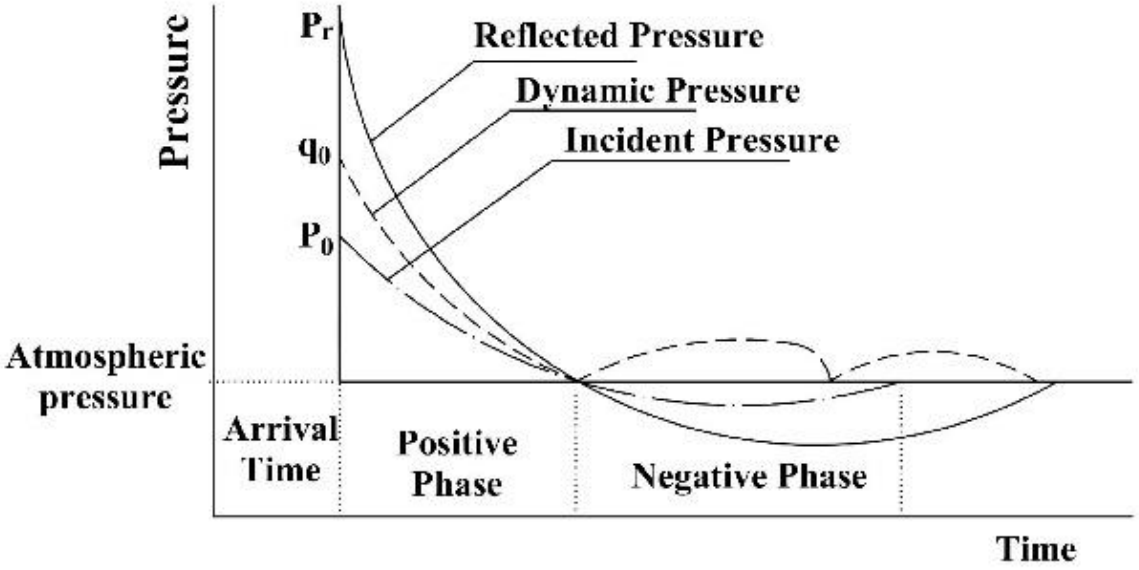

Figure 4 Variation of blast pressure over time

Previous studies

Yang et al., (2023) examined how urban bridges respond to far-field blast loads using numerical simulations. These blasts produce long-duration waves, leading to unique damage patterns. Using the Autodyne subroutine, they validated their model with experiments. The study found that far field blasts because global bridge effects, like pier tilt and superstructure uplift, with damage to piers, shear keys, and superstructures. Lower impact angles increase pier displacement and reduce superstructure uplift, with peak overpressure being crucial. This research informs urban safety and helps engineers mitigate blast impacts. Lin et al., (2023) investigated the effects of blast loads on the damage and remaining strength of strand cables. This study, conducted at Southeast University, offers vital insights into the performance of civil engineering materials under extreme conditions.

The researchers pinpointed failure mechanisms and evaluated the residual capacity of the cables after blast exposure. Their findings underscore important considerations for the design and safety assessment of structures using strand cables, especially in contexts involving explosive threats, and highlight the importance of understanding material behavior to enhance structural resilience. Maiorana et al., (2022) investigated the effect of blast loads on the structural integrity of steel arch bridge slabs using advanced numerical simulations. Their analysis revealed that blast loads significantly compromise the slabs, causing various forms of damage such as cracking, spalling, and deformation. The study emphasized the need for incorporating blast resistance in the design and maintenance of steel arch bridges to ensure resilience against such extreme events. These findings provide critical insights for civil engineers and urban planners in enhancing the safety and durability of essential infrastructure.

Anas et al., (2022) examined the impact response of square reinforced concrete (RC) slabs with normal strength concrete, focusing on different strengthening methods. Their study assesses the performance of slabs reinforced with laminates of mild steel and carbon-fiber reinforced polymer (C-FRP), as well as those with C-FRP strips, under falling-weight impact loads. The research, through both numerical simulations and experimental tests, provides insights into how these reinforcement techniques enhance the impact resistance and overall structural performance of the slabs. Tahzeeb et al., (2022) conducted a numerical study comparing the performance of composite and tubular columns under close-in blast loading. Their research found that composite columns offer superior energy absorption and resistance to deformation compared to tubular columns. This study highlights the effectiveness of composite designs in enhancing structural resilience against blast forces, providing valuable insights for optimizing blast-resistant column design.

Zhu et al., (2020) studied the damage mechanisms of a multi-beam steel-concrete composite bridge under a car explosion, using a 50 kg TNT equivalent to simulate the explosion. They found that the bridge undergoes three failure stages: elastoplastic, plastic, and a plastic hinge with a whole section. Failure times and displacements vary depending on whether the explosion occurs above the steel beams or the concrete deck. The study found that explosions occurring from the bearings to one-quarter of the bridge span lead to

shear failure in steel beams before bending failure. Both shear and bending failures are important considerations for designing explosion-resistant structures. For explosions between one-quarter and one-half of the bridge length, flexural failure becomes the main factor affecting the damage to the steel–concrete composite bridge, with only localized shear failure occurring. In a multi-beam steel–concrete composite bridge that meets design specifications, any explosion will result in the formation of plastic hinges and a loss of bearing capacity.

Amer et al., (2019) investigated the behavior of a simply supported composite steel I-girder bridge under blast loads. They placed three different explosive sizes at various locations above the deck. The researchers found that steel girder failure primarily causes the bridge collapse, while reinforced concrete slabs do not lead to collapse. They observed a total collapse in the girder directly above the blast when the explosive weight reached 5000 kg. Hashemi et al., (2017) studied the dynamic response of a cable-stayed bridge under blast load. This study develops detailed finite element models of a steel cable-stayed bridge and analyzes them using an explicit solver. The researchers use three explosive sizes, small, medium, and large, and place them above the deck. The researchers concluded that although they observed extensive damage and steel plate rupture, along with large plastic deformations and strains in the tower and deck in some blast scenarios, the damage did not cause global progressive failure deck or tower in any of the scenarios considered.

The bridge did not collapse gradually under varying blast loads from minor to big explosions; however, major repairs and rehabilitation would be necessary for structural elements like the deck and towers near the explosion. Cofer et al., (2012) studied the effects of blast loading on pre-stressed girder bridges using a finite element model validated by experimental tests. The study expanded the model to a four-girder bridge and examined three scenarios: A blast between girders above the deck, a blast centered on a girder above the deck, and a blast beneath the deck. Blasts from above caused localized damage, making it possible to reopen other sections of the bridge immediately after the event. In contrast, a blast from below severely damaged the slab but left the girders intact. Tokal-Ahmed, (2009) studied the response of concrete I-girder bridges to blast loads, revealing that the standoff distance and charge weight are crucial factors. The distribution of blast pressure along the bridge significantly influences its behavior.

At larger standoff distances, the pressure distribution tends to be uniform, while at smaller distances, it can lead to potential overestimation of the effects. The study also found that when the member's length exceeds the standoff distance, the pressure at the ends increases significantly, approaching incident pressure. The study also examined how the standoff distance affects the reflected pressure on the bridge span. Based on previous studies, there is limited research on the behavior of composite steel box girder bridges under blast effects. The existing research does not sufficiently address the various parameters that might influence this behavior. Therefore, this research aimed to study the dynamic behavior of steel box girder bridges exposed to blast loads and the parameters that might affect this behavior, such as explosive weight, blast standoff distance, and blast location. Additionally, the research explored the possibility of partially reopening the bridge for traffic after the explosion.

2. METHODOLOGY

Overview of the Study Building

This study used a composite steel box girder bridge with a 30-meter span and a 10-meter-wide concrete deck, as shown in (Figure 5). The model restrained the bridge at both ends with hinge and roller supports. The design assumed the bridge would accommodate two traffic lanes. The design followed the Egyptian Code ECP-201, (2012) for live load, dead load, and impact load to determine the steel girder cross-section and concrete slab reinforcement details. The concrete slab reinforcement included Φ25/150 mm for the transversal direction and Φ16/200 mm for the longitudinal direction. Figure 6 shows the dimensions of the steel box girder.

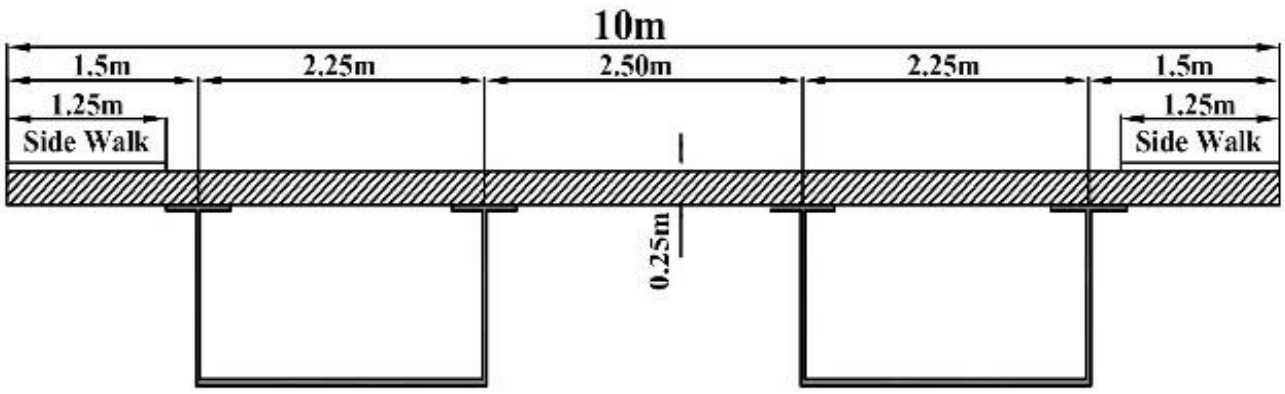

Figure 5 Cross section of the study bridge

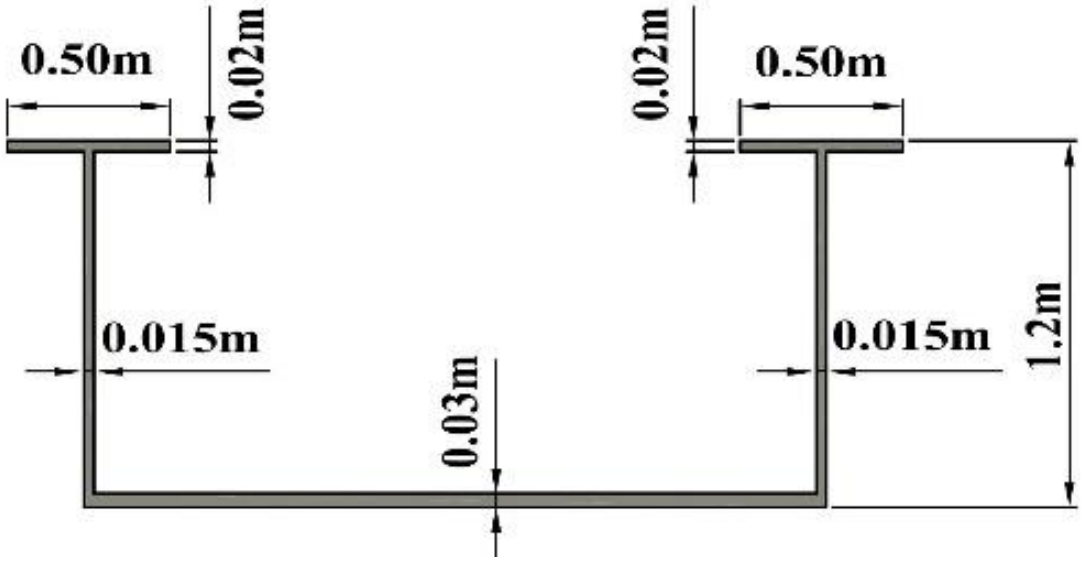

Figure 6 Steel box girder dimensions

Materiel properties

Concrete

The study used the concrete damage plasticity (CDP) model to simulate the non-linear behavior of concrete. The CDP model includes two main failure modes: Tensile cracking and compressive crushing, as shown in Figure 7 (Long and He, 2017). The study adopted concrete grade B40, which has a cubic strength of 40 MPa. Table 2 Hafezolghorani et al., (2017) presents the parameters for the concrete damage plasticity model, including the damage parameter, strain hardening and softening rules, and other elements.

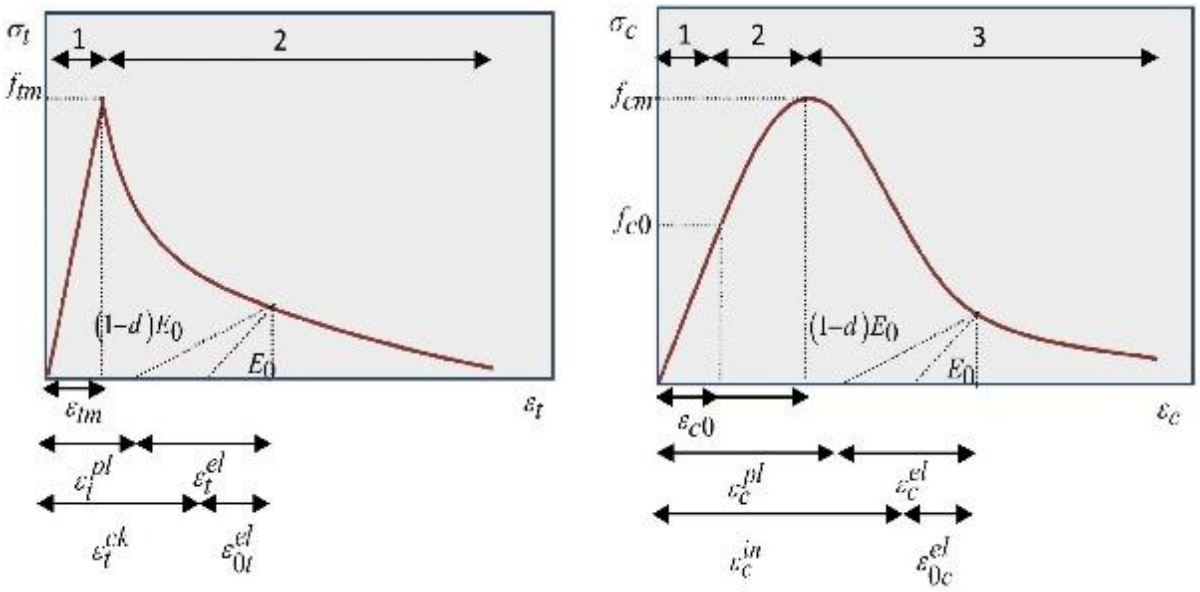

Figure 7 Concrete response to a uniaxial loading condition

Table 2 Material properties for concrete with CDP model in class B40

Concrete elasticity		**Plasticity parameters**	
Young's modulus (GPa)	30	Dilation angle	31
Poisson's ratio	0.20	Eccentricity	0.1
Mass Density (Kg/m3)	2500	Viscosity Parameter	0
Concrete compressive behavior		Concrete compressive damage	
Yield stress (MPa)	Inelastic strain	Damage parameter	Inelastic strain
20.40	0	0	0
25.60	2.6667E-05	0	2.6667E-05
30	0.00008	0	0.00008
33.60	0.00016	0	0.00016
36.40	0.00026667	0	0.00026667
38.40	0.0004	0	0.0004
39.60	0.00056	0	0.00056
40	0.00074667	0	0.00074667
39.60	0.00096	0.01	0.00096
38.40	0.0012	0.04	0.0012
36.40	0.00146667	0.09	0.00146667
33.60	0.00176	0.16	0.00176
30	0.00208	0.25	0.00208
25.60	0.00242667	0.36	0.00242667
20.40	0.0028	0.49	0.0028
14.40	0.0032	0.64	0.0032
7.60	0.00362667	0.81	0.00362667
Concrete tensile behavior		Concrete tension damage	
Yield stress (MPa)	Cracking strain	Damage parameter	Cracking strain
4	0	0	0
0.04	0.0013333	0.99	0.0013333

Steel

Due to the instantaneous and high-energy nature of the explosion load, the structure's response causes the material to exhibit high strain rate characteristics (Lin et al., 2012; Bobbili and Madhu, 2017; Asala et al., 2019). Many researchers have examined the steel constitutive model under blast loads and found that the Johnson-Cook (JC) model accurately simulates the strain rate sensitivity and thermal softening of steel. Equation (1) provides a detailed description of this model. The study chose Steel S355 for both rafters and reinforcement bars. Table 3 lists the parameters for S355 (Forni et al., 2016).

$$\sigma = (A + B\,\varepsilon pn)\,(1 + C \ln \varepsilon p^*) \quad (1)$$

Where σ is the Von Mises stress, A is the yield stress under the static loading condition, B is the hardening constant, C is the strain rate constant, εp is the effective plastic strain, n is the strain hardening coefficient, and εp* is the normalized effective plastic strain rate.

Table 3 Model parameters for steel.

A (MPa)	B (MPa)	C	n
448	782	0.024	0.56

Define loads

Dead load refers to the weight of all the bridge's components, determined by its design and geometry. The typical density for concrete material is 2500 kg/m³, and for steel material, it is 7850 kg/m³. According to the Egyptian Code for Loads, ECP 201, (2012), the design live load consists of concentrated vehicle loads and distributed loads along the span length. The distributed uniform load also varies across the width of the bridge. Figure 8 shows the selected configuration for the traffic load. Since our study focuses on a two-traffic-lane bridge, we will adopt two vehicle weights, 60 tons and 40 tons, and the relevant distributed load.

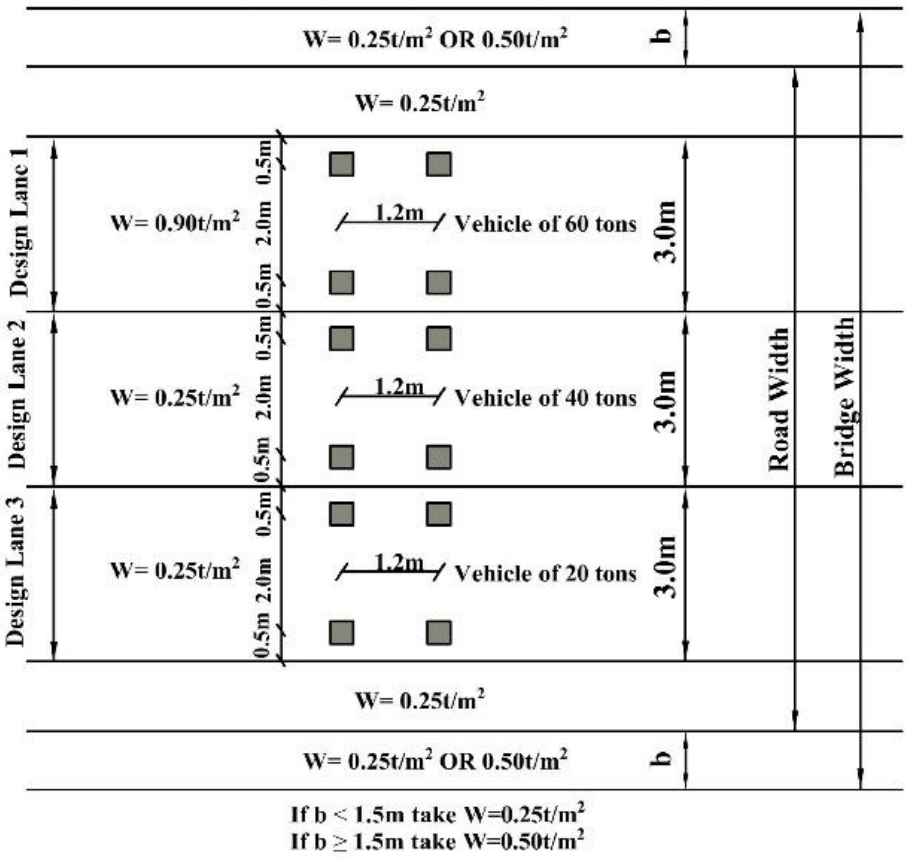

Figure 8 Loading configuration for a typical bridge width as specified by ECP 201-2012

The study placed detonation points for explosives at various locations to maximize their impact on bridge elements. Transversally, the study positioned the points between the two girders and directly above one girder. Longitudinally, the blasts occur at the mid-span and at the end-span. The study used standoff distances of 1.0 m, 1.5 m, and 2.0 m. It applied various explosive weights to represent different blast conditions: 50 kilograms (motorcycle), 200 kilograms (medium car), 300 kilograms (large car), 1400 kilograms (pick-up truck), 3000 kilograms (van), and 5000 kilograms (truck), based on the loading capacity of different vehicles. Figure 9 shows the detonation points adopted in the study.

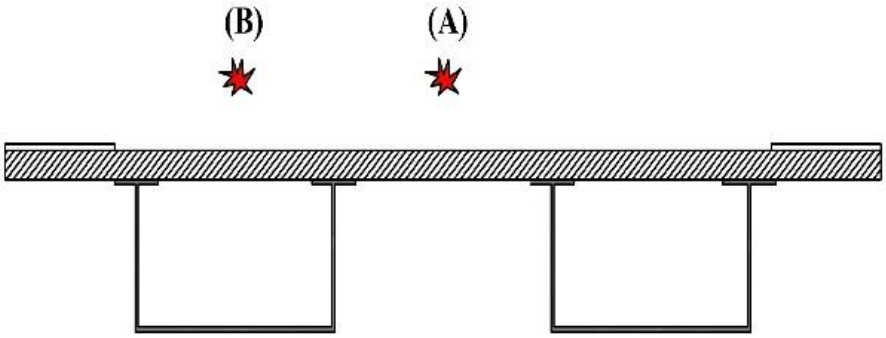

Figure 9 Detonation points along bridge cross-section.

Finite element analyses

This study used ABAQUS nonlinear finite element analysis software to model the bridges. The study modeled concrete slabs with solid elements, steel box girders with mesh elements, and the deck system reinforcement with truss elements. Additionally, the study made the girders composite with the concrete slab during the nonlinear analysis, as shown in (Figure 10). Table 4 lists the different load cases used in the analysis models.

Figure 10 Model for the composite steel box girder bridge using ABAQUS

Table 4 List of multi-case bridge loading

Explosive weight (kg)	Blast location	Standoff distance (m)	Number analysis of bridge
(50, 200, 300, 1400, 3000, 5000)	Centered above girder at mid-span	(1, 1.5, 2)	18
(50, 200, 300, 1400, 3000, 5000)	Centered in between girders at mid-span	(1, 1.5, 2)	18
(50, 200, 300, 1400, 3000, 5000)	Centered above girder at end-span	(1, 1.5, 2)	18
(50, 200, 300, 1400, 3000, 5000)	Centered in between girders at end-span	(1, 1.5, 2)	18
Total number of bridges:			Ridges

3. RESULTS AND DISCUSSION

The study used finite element modelling for an extensive parametric analysis to explore how various parameters affect the behavior of composite steel box girder bridges subjected to blast loads. The parameters examined include explosive weight, blast standoff distance, and explosion location. The analysis revealed two primary failure modes. For a blast at mid-span, the bridge experienced bending failure because the bending stress exceeded the bending capacity of the bridge elements.

This failure mode involved initial cracking of the concrete slab, yielding of the tensile reinforcement, compression failure of the concrete slab, and yielding of the steel girders. For a blast at the span end, the bridge suffered shear failure near the supports because the applied shear stress surpassed the shear capacity of the bridge elements. The models showed that part of the reinforced concrete slab and some steel girders reached the failure stage, depending on the loading cases of the bridge. The following section details how each parameter affects the behavior of composite steel box girder bridges under blast loads.

Effect of each parameter on the behavior of a composite steel box girder bridge subjected to blast load

Explosive weight

In this study, we tested various explosive weights to assess the bridge's behavior and examine both minor and severe effects, matching the explosive weights to the loading capacities of different vehicles. Results from ABAQUS software revealed that the blast created a hole in the deck slab as the concrete and reinforcement reached their ultimate capacity. The extent of collapse in the reinforced concrete directly correlated with the explosive weight (W), as shown in (Figure 11 and 12). Similarly, the collapse of the steel box girder also directly correlated with the explosive weight (W), as illustrated in (Figure 13 and Table 5). The bridge collapsed when exposed to an explosive weight of 5000 kilograms (truck). These results align with recent research on the effects of explosive weights on the dynamic behavior of bridges. For example, Aamir et al., (2023) studied the effect of different explosive weights on a steel highway girder bridge and found similar results, confirming the robustness and accuracy of our current models.

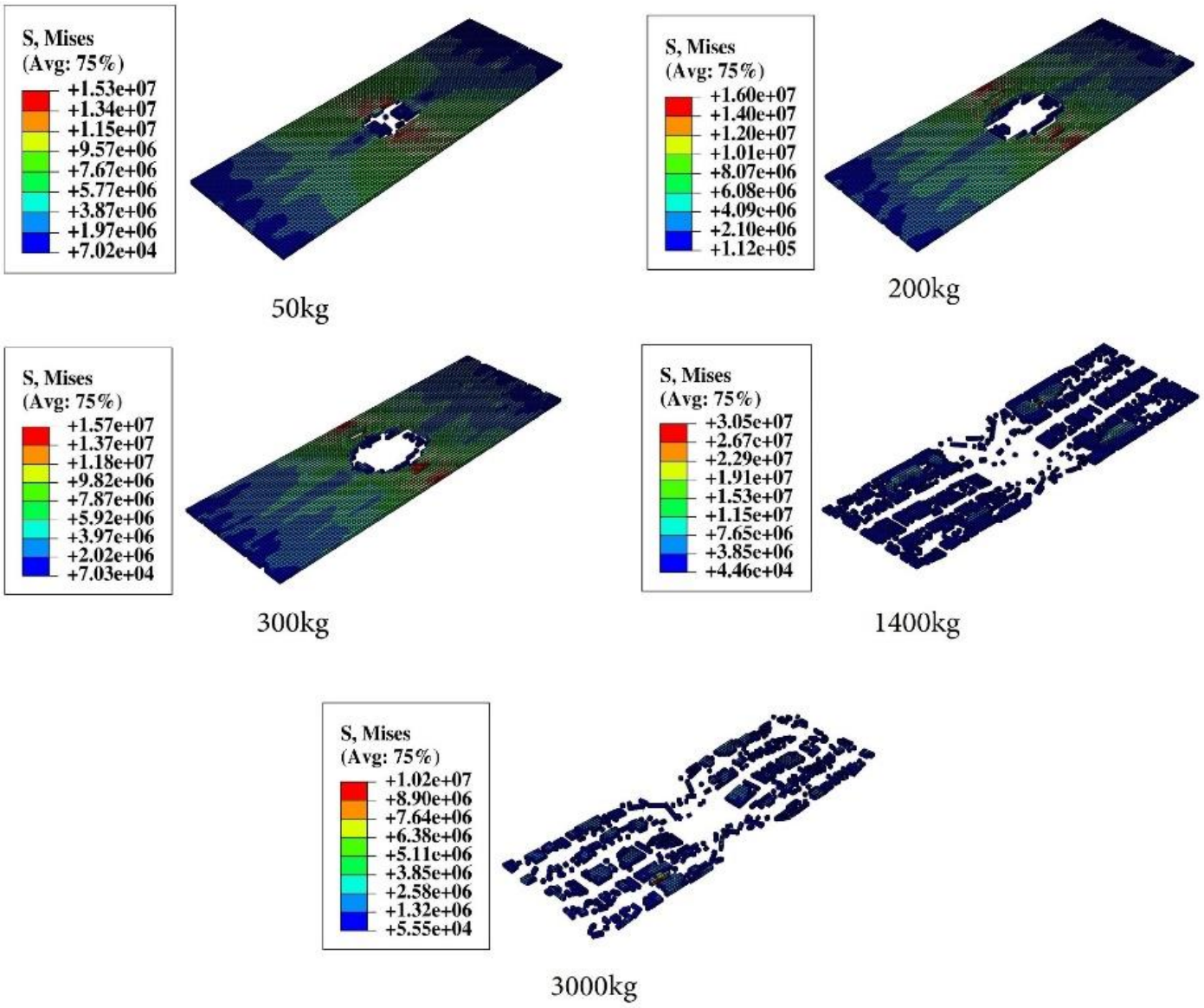

Figure 11 Area collapsed in concrete slab subject to various explosive weights (mid-span, between girders, R = 1.0m)

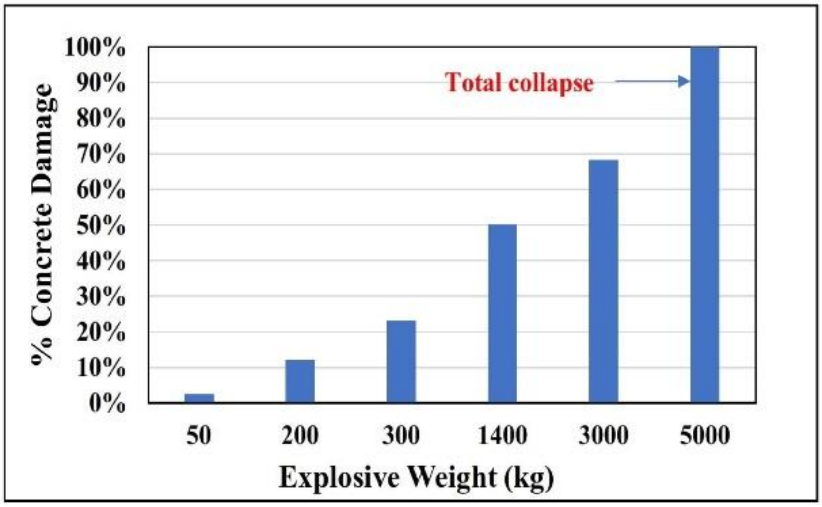

Figure 12 Percentage of damage to the concrete slab area under various explosive weights (mid-span, between girders, R = 1.0m)

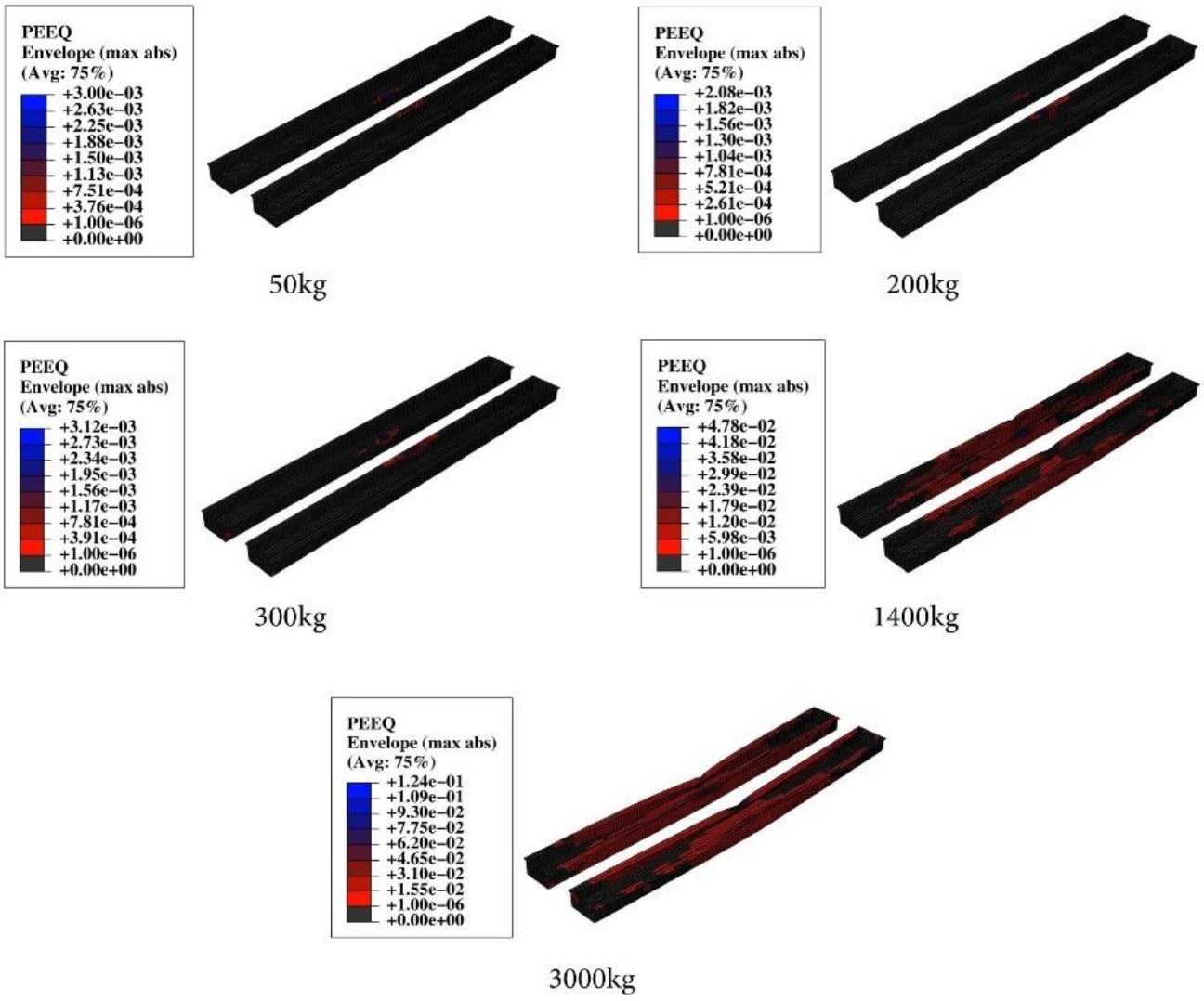

Figure 13 Plastic strain of box girder subject to various explosive weights (mid-span, between girders, R = 1.0m)

Table 5 State of box girder subject to various explosive weights (mid-span, between girders, R = 1.0m)

Explosive weight	State of steel box girder
50Kg (Motorcycle)	No plastic strains formed
200Kg (Medium Car)	No plastic strains formed
300Kg (Large Car)	plastic strains formed at the top flanges only
1400Kg (Pick-up truck)	plastic strains formed at the top flanges and part of the height of the web
3000Kg (Van)	plastic strains formed at the top flanges and total height of the web
5000Kg (Truck)	Complete plastic hinge formed (total collapse)

Blast Standoff Distance

In this study, we used different standoff distances (R) to predict the bridge's behavior under blast loads and examine both minor and major effects. We tested standoff distances of 1.0 m, 1.5 m, and 2.0 m. Results from ABAQUS software showed that the effect of changing the standoff distance depends on the explosive weight. For smaller weights (50 kg, 200 kg, 300 kg), increasing the standoff distance reduces the blast effect on all bridge elements. For larger weights (1400 kg, 3000 kg, 5000 kg), it causes a more widespread impact on the bridge. For example, with a 300 kilograms charge, increasing the standoff distance from 1 m to 2 m decreased the damaged concrete area from 23% to 18% of the total slab area and eliminated plastic strains in the steel girders, which initially formed only at the top flanges.

Conversely, with a 1400 kilograms charge, increasing the standoff distance from 1 m to 2 m increased the damaged concrete area from 50% to 65% of the total slab area and extended plastic strains in the steel girders from the top flanges and part of the web height to the top flanges and the entire web height. Figures 14, 15, 16, and 17 show the failure of both concrete and steel at different standoff distances for charge weights of 300 kilograms and 1400 kilograms, respectively. Figure 18 illustrates the concrete damage at different standoff distances, showing how a larger load with a greater standoff distance has a more severe impact on the concrete slab. Table 6 summarizes the blast effect on the steel box girder. These results are consistent with recent research on the effect of standoff distance on the dynamic behavior of bridges subjected to blast loads. A study by Amer et al., (2019) on the effect of standoff distance on a composite steel I-girder bridge found similar results, demonstrating the strength and correctness of our current models.

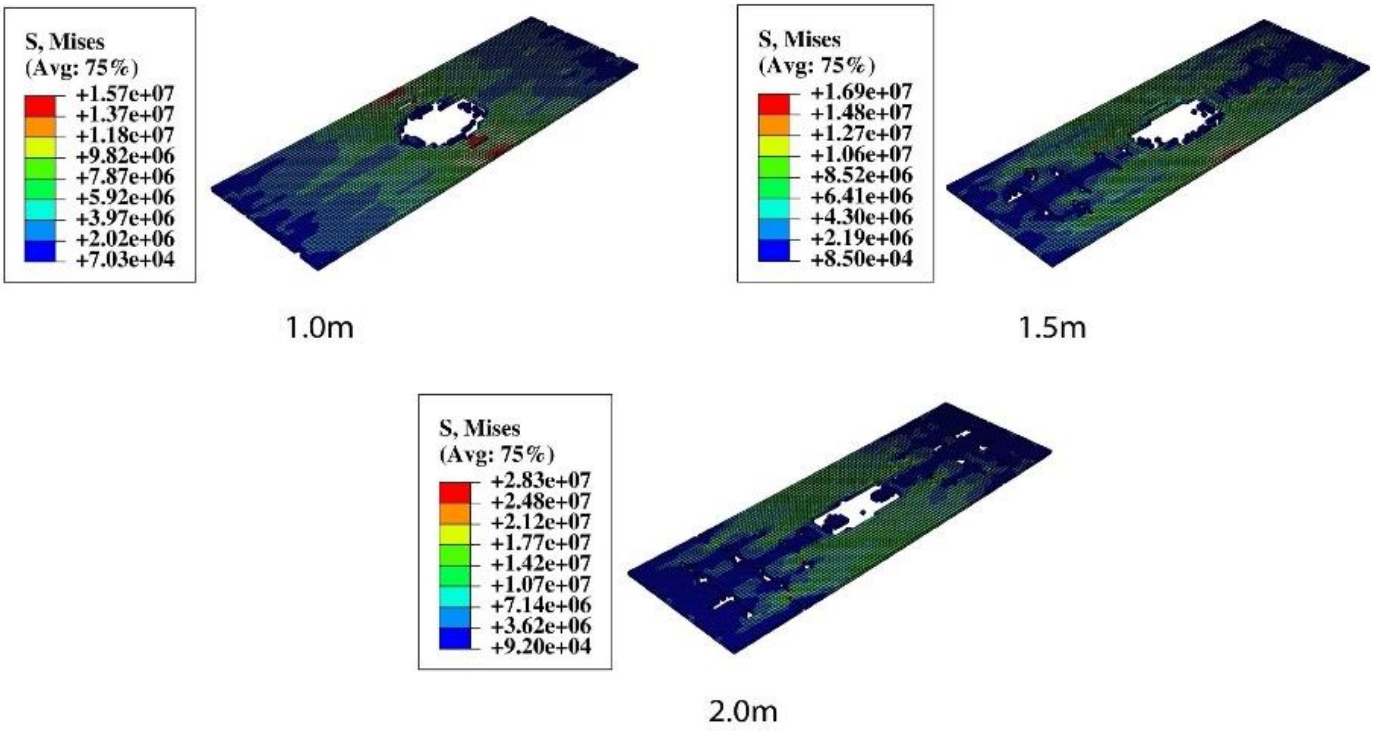

Figure 14 Area collapsed in concrete slab subject to various blast standoff distances (mid-span, between girders, W = 300Kg)

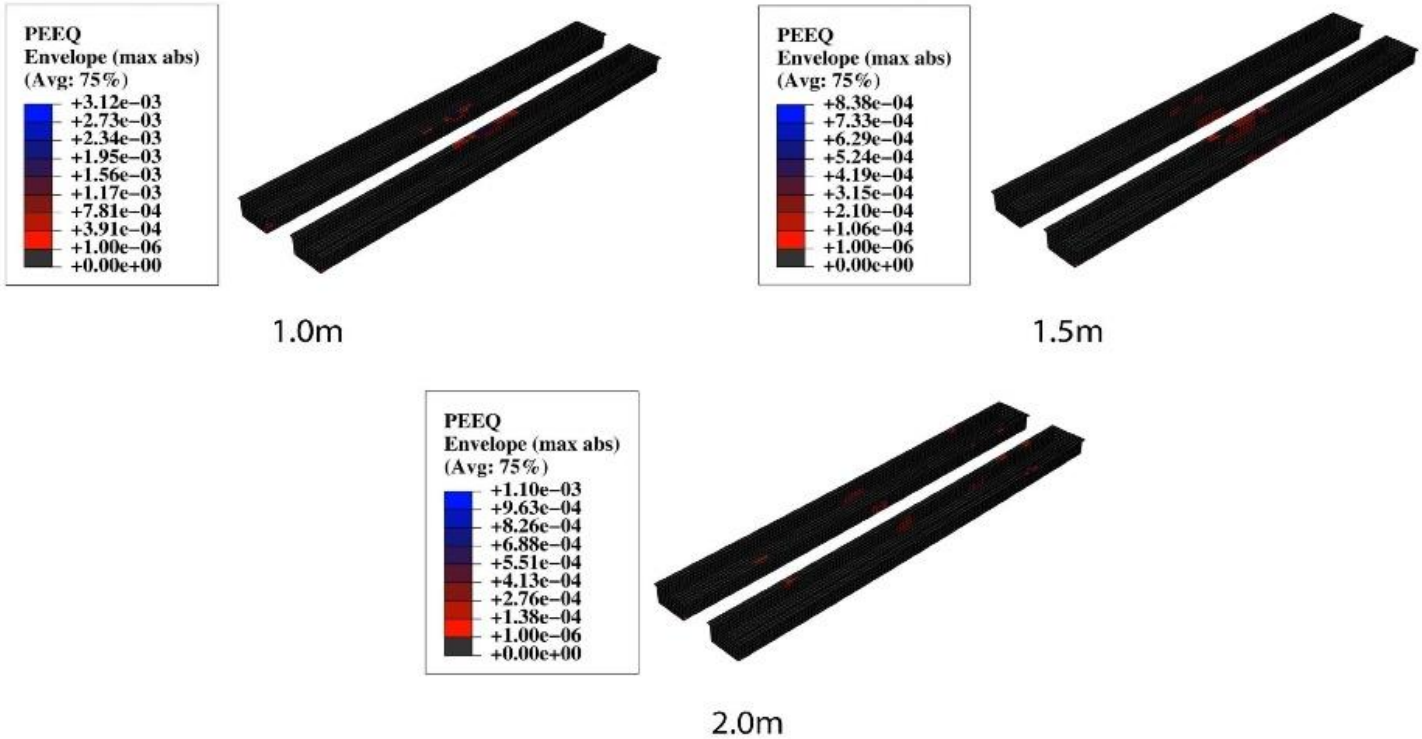

Figure 15 Plastic strain of box girder subject to various blast standoff distances (mid-span, between girders, W = 300Kg)

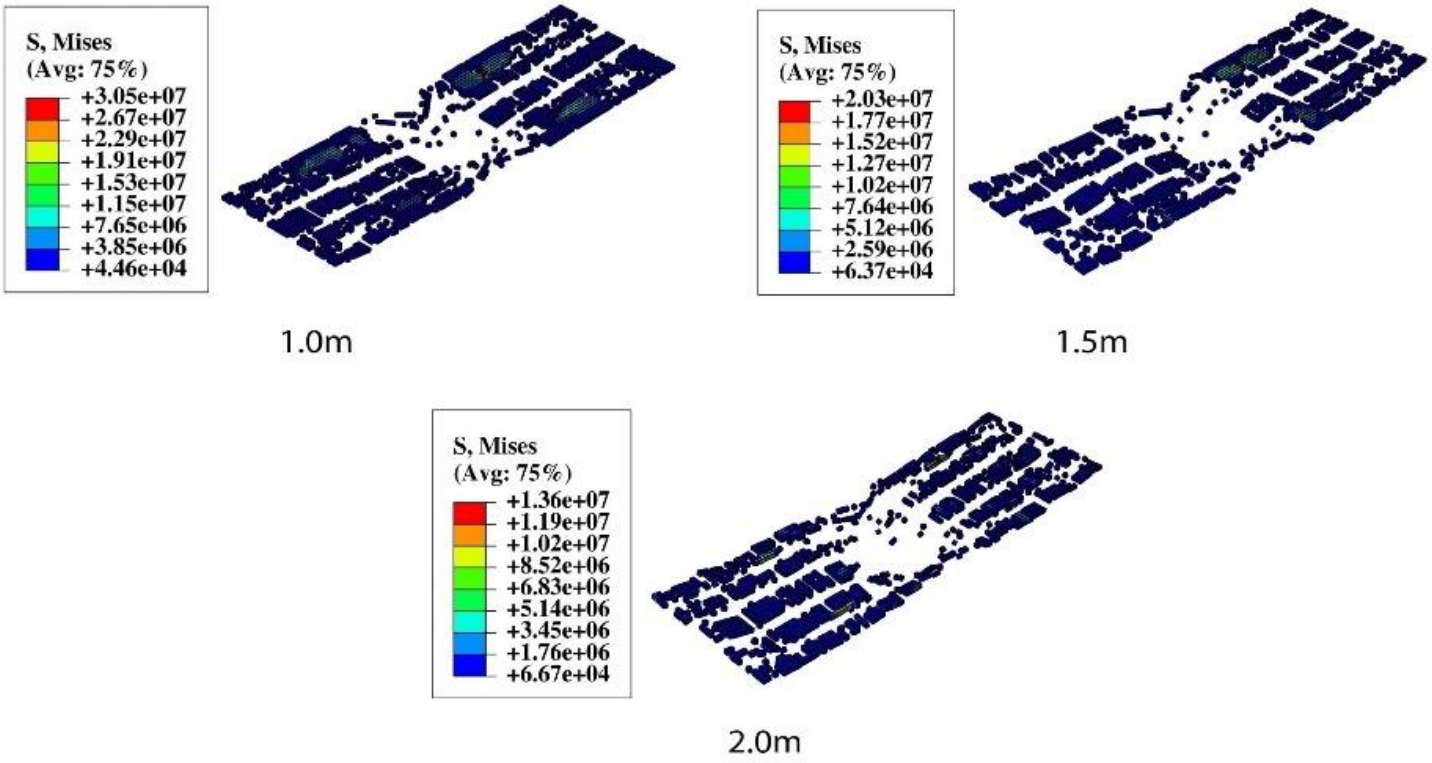

Figure 16 Area collapsed in concrete slab subject to various blast standoff distances (mid-span, between girders, W = 1400Kg)

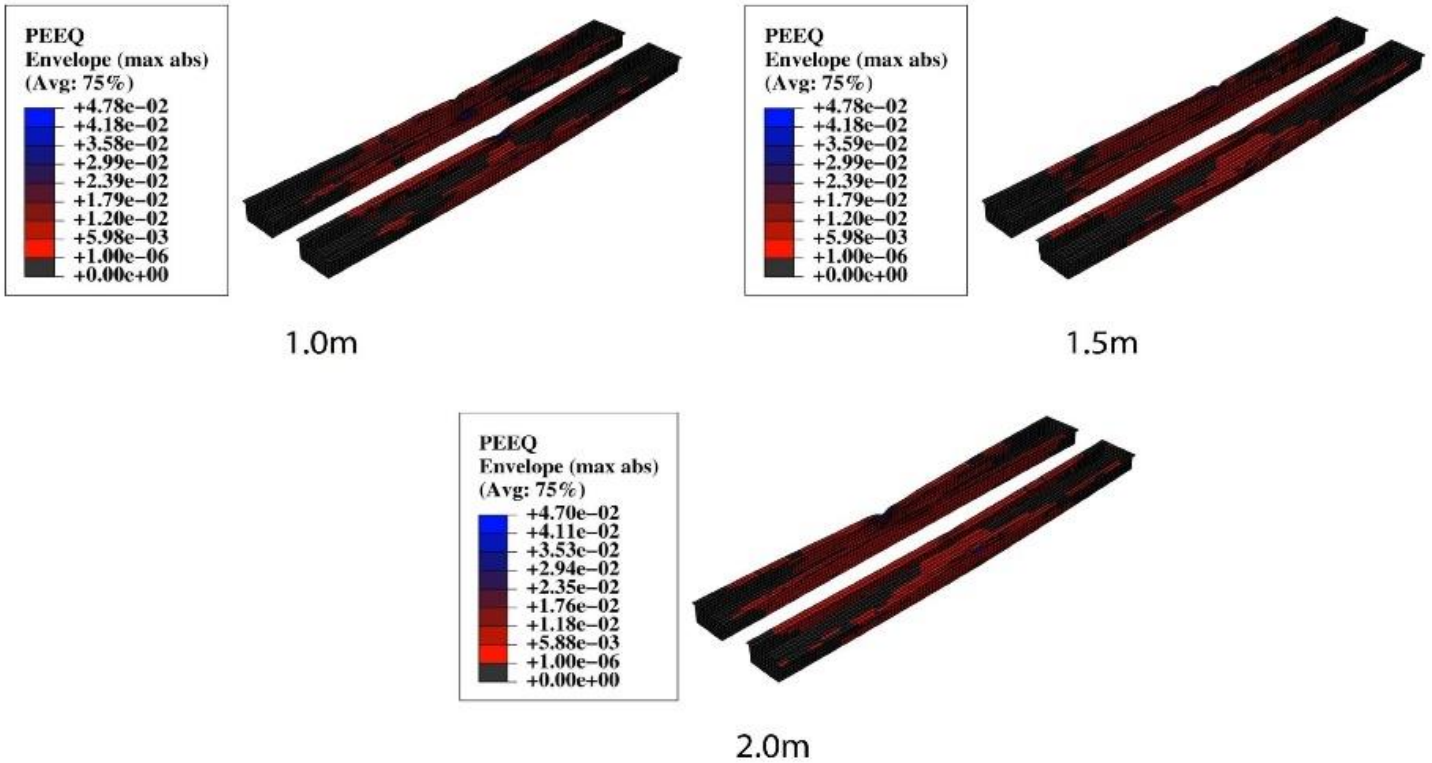

Figure 17 Plastic strain of box girder subject to various blast standoff distances (mid-span, between girders, W = 1400Kg)

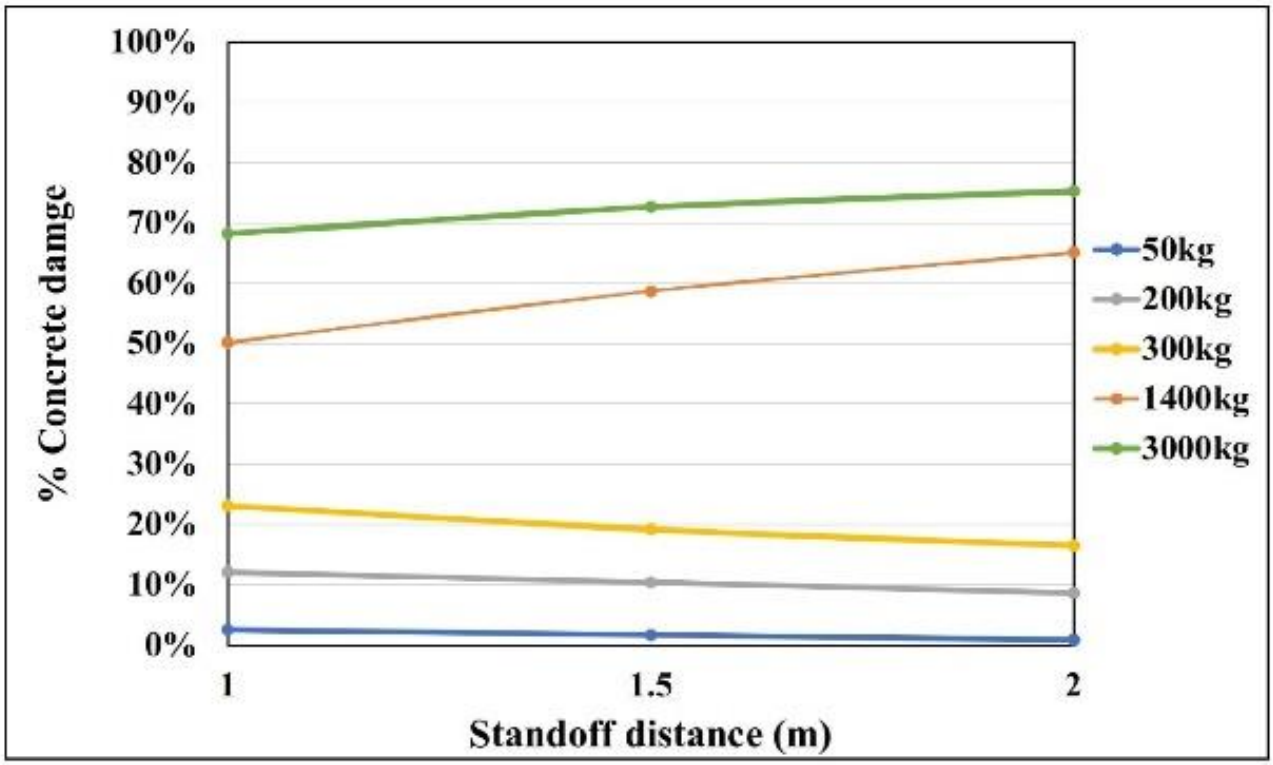

Figure 18 Percentage of damage to the concrete slab area subject to various blast standoff distances (mid-span, between girders)

Location of explosion

In this study, we evaluated the bridge's response to blast loads by testing four different explosion locations: mid-span centered between girders, mid-span centered above girders, end-span centered between girders, and end-span centered above girders. Results from ABAQUS software showed that explosions at mid-span, especially when centered between girders, are more likely to cause failure in reinforced concrete slabs, as seen in (Figure 19 and 20). In contrast, explosions at the span end are more likely to cause failure in steel box girders, as shown in (Figure 21 and Table 7). These results are consistent with current research into the effect of explosion location on bridge dynamics. Aamir et al., (2023) investigated the impact of several explosion locations on steel highway girder bridges and observed the same findings, validating the robustness and correctness of our present models.

Table 6 State of box girder subject to various blast standoff distance (mid-span, between girders)

Explosive weight	Standoff distance (m)	State of steel box girder
300Kg (Large Car)	1.0	Plastic strains formed at the top flanges only
300Kg (Large Car)	1.5	No plastic strains formed
300Kg (Large Car)	2.0	No plastic strains formed
1400Kg (Pick-up truck)	1.0	Plastic strains formed at the top flanges and part of the height of the web
1400Kg (Pick-up truck)	1.5	Plastic strains formed at the top flanges and Part of the height of the web

1400Kg (Pick-up truck)	2.0	Plastic strains formed at the top flanges and total height of the web

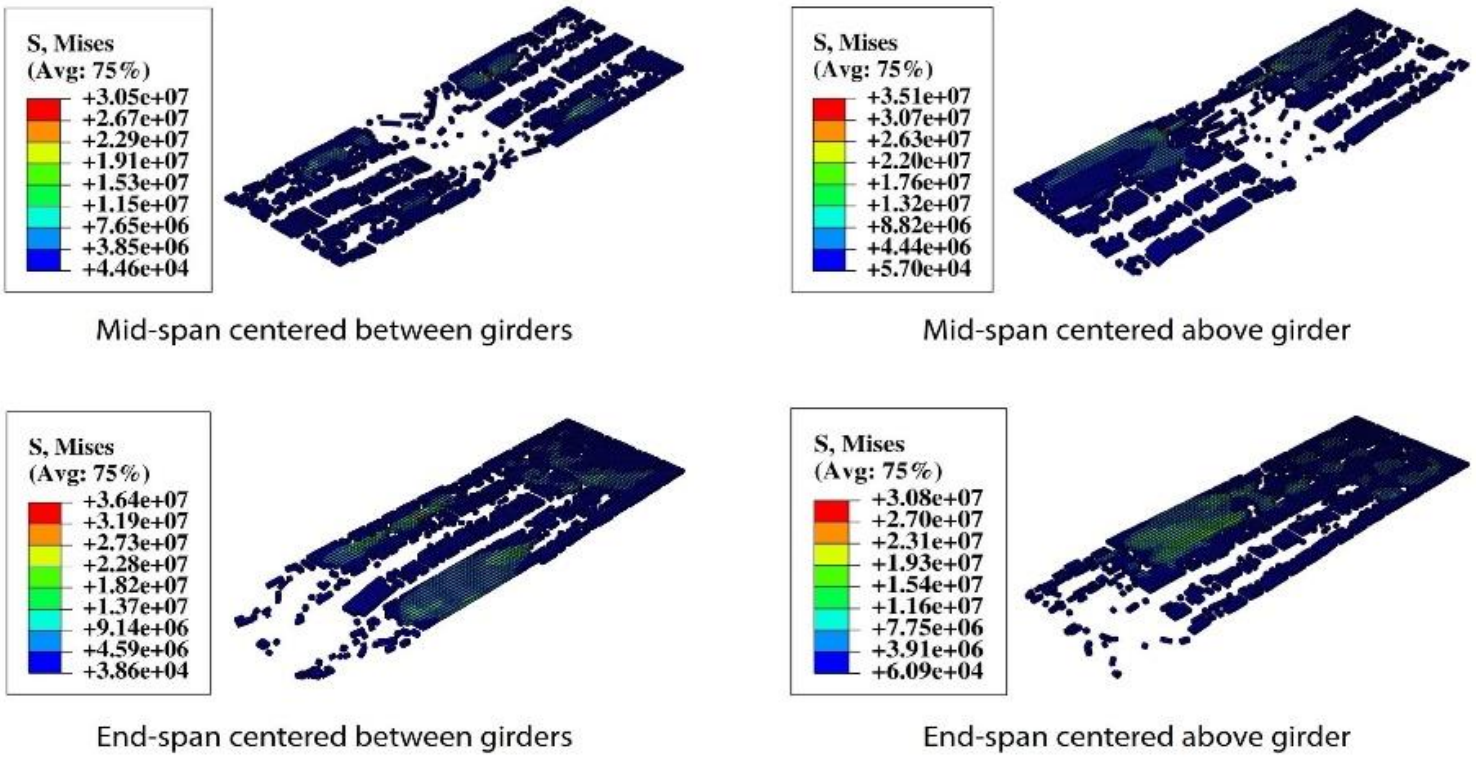

Figure 19 Area collapsed in concrete slab subject to various locations of explosion (W = 1400Kg, R= 1.0m)

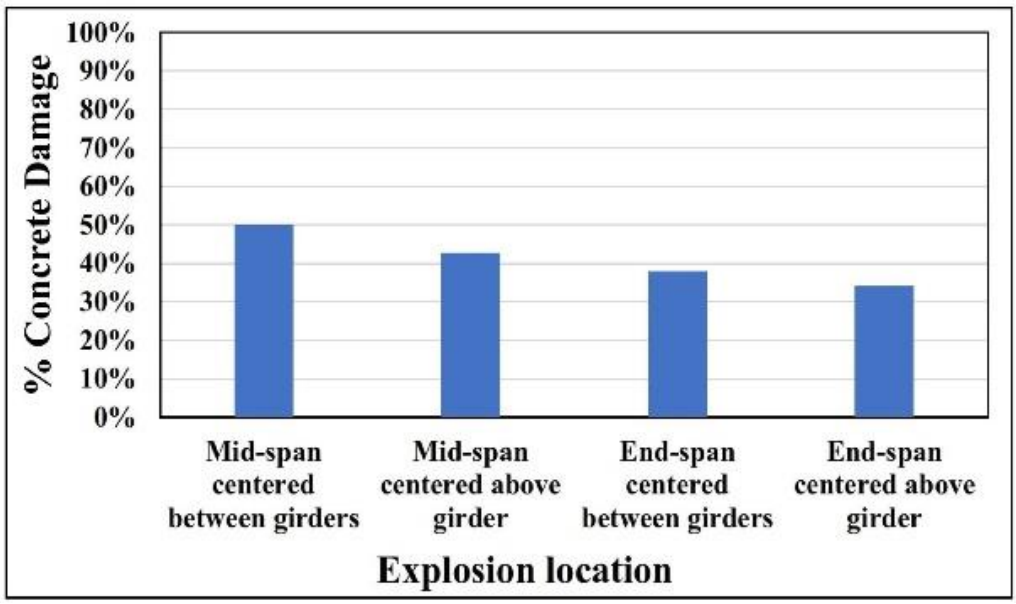

Figure 20 Percentage of concrete slab damage area subject to various locations of explosion (W = 1400Kg, R= 1.0m)

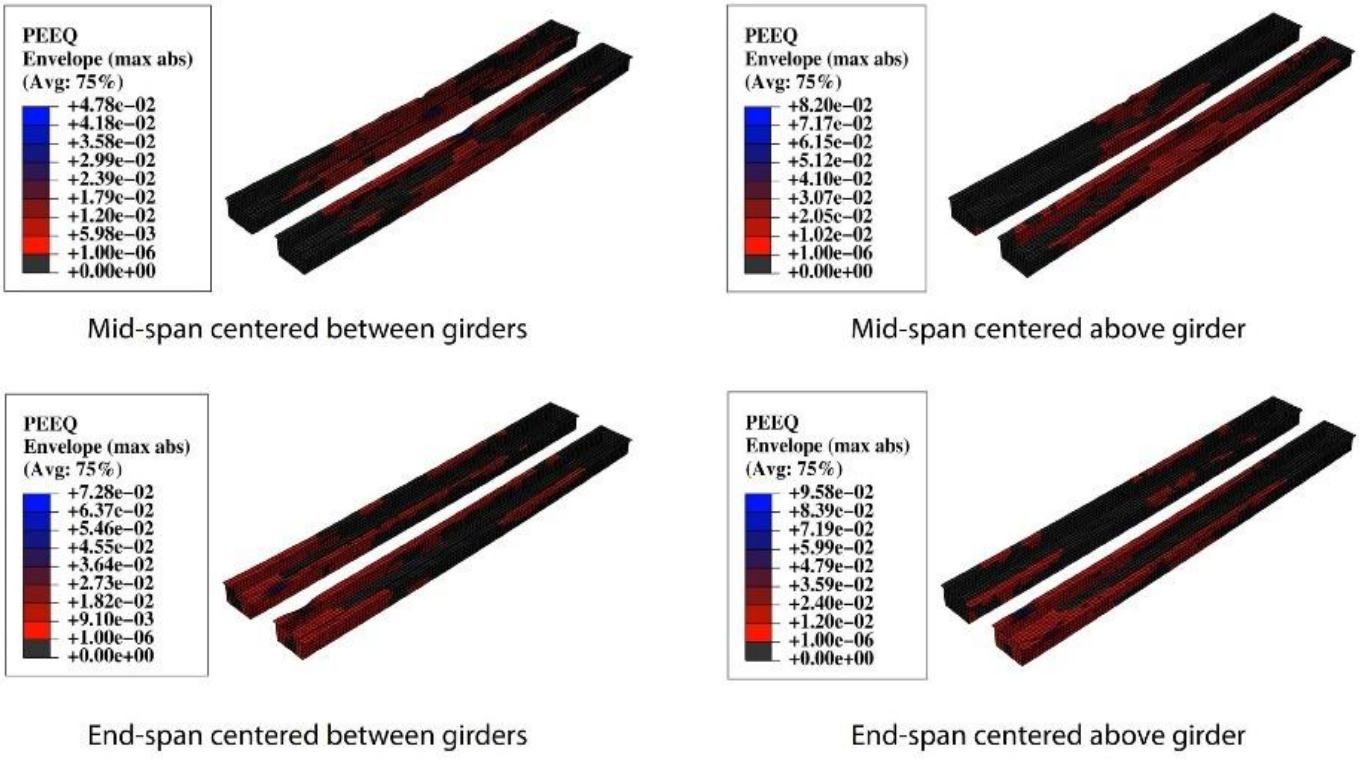

Figure 21 Plastic strain of box girder subject to various locations of explosion (W = 1400Kg, R= 1.0m)

Table 7 State of steel box girder subject to various location of explosion (W = 1400Kg, R= 1.0m)

Explosion location	State of steel box girder
Mid-span centered between girders	Plastic strains formed at the top flanges and part of the height of the web
Mid-span centered above girder	Plastic strains formed at the top flanges and part of the height of the web
End-span centered between girders	Plastic strains formed at the top flanges and total height of the web
End-span centered above girder	Plastic strains formed at the top flanges and total height of the web

Possibility of reopening the bridge partially for traffic after the explosion

This section examines the possibility of reopening other bridge sections after an explosion. The process involves first evaluating bridge's width where deflection remains within the allowable limit after the blast. This width then compared to the standard traffic lane width, which is 3.0 m according to the Egyptian code for design loads on roadway bridges. If the width of the bridge with permissible deflection exceeds the traffic lane width, reopening that section of the bridge is possible. Otherwise, reopening is not feasible. Table 8 shows the potential for reopening the bridge after an explosion.

Table 8 The possibility of reopening the bridge is subject to various explosive weight

Explosive weight (W)	Standoff distance (R)	Explosion location (Midspan)		Explosion location (Endspan)	
		Between girders	Above girder	Between girders	Above girder
50Kg (Motorcycle)	1.0m, 1.5m, 2.0m	The slab was locally damaged, allowing to reopen the bridge partially		The slab was locally damaged, allowing to reopen the bridge partially	
200Kg (Medium Car)	1.0m, 1.5m, 2.0m	The slab was locally damaged, allowing to reopen the bridge partially		The slab was locally damaged, allowing to reopen the bridge partially	
300Kg (Large Car)	1.0m, 1.5m, 2.0m	The slab was severely damaged, making it impossible to reopen the bridge partially		The slab was severely damaged, making it impossible to reopen the bridge partially	
1400Kg (Pick-up truck)	1.0m, 1.5m, 2.0m	The slab was severely damaged, making it impossible to reopen the bridge partially		The slab was severely damaged, making it impossible to reopen the bridge partially	
3000Kg (Van)	1.0m, 1.5m, 2.0m	The slab was severely damaged, making it impossible to reopen the bridge partially		The slab was severely damaged, making it impossible to reopen the bridge partially	
5000Kg (Truck)	1.0m, 1.5m, 2.0m	Total collapse of bridge		Total collapse of bridge	

4. CONCLUSION

This research investigates the dynamic behavior of steel box girder bridges when exposed to blast loads, focusing on factors like explosive weight, blast standoff distance, and blast location. It also explores the possibility of partially reopening the bridge to traffic immediately after an explosion. The study concludes that the collapsed area in reinforced concrete and steel box girders is directly proportional to the explosive weight. Partial collapses occur under explosive weights of 50 kilograms (motorcycle), 200 kilograms (medium car), 300 kilograms (large car), 1400 kilograms (pick-up truck), and 3000 kilograms (van), while an explosive weight of 5000 kilograms (truck) causes complete collapse. The effect of changing the standoff distance depends on the explosive weight. Increasing the standoff distance for smaller weights (50 kg, 200 kg, 300 kg) reduces the blast effect. For larger weights (1400 kg, 3000 kg, 5000 kg), it causes a more widespread impact.

For example, with a 300-kilogram charge, increasing the standoff distance from 1 m to 2 m decreased the damaged concrete area from 23% to 18% and eliminated plastic strains in the steel girders. Conversely, with a 1400 kilograms charge, increasing the standoff distance from 1 m to 2 m increased the damaged concrete area from 50% to 65% and extended plastic strains in the steel girders from the top flanges to the entire web height. In all cases, a mid-span blast causes more frequent failure of reinforced concrete slabs, especially when the blast occurs between girders, while steel box girders are more likely to fail from a blast at the span ends. Explosive weights of 50 kilograms (motorcycle) and 200 kilograms (medium car) caused localized damage, allowing for the possibility of reopening other sections of the bridge immediately after the explosion. However, explosive weights of 300 kilograms (large car), 1400

kilograms (pick-up truck), and 3000 kilograms (van) severely damaged the bridge, making partial reopening impossible without risking complete collapse.

Acknowledgements
We thank Dr. Kamel Tamer for his helpful advice on various technical issues examined in this paper

Author Contributions
All authors contributed to the study conception and design. Ahmed Z Hanafi and Ahmed H Amer performed material preparation, data collection and analysis. Walid A Attia wrote the first draft of the manuscript. All authors read and approved the final manuscript.

Ethical Issues
Not applicable.

Informed consent
Not applicable.

Funding
This study has not received any external funding.

Conflict of Interest
The author declares that there are no conflicts of interests.

Data and materials availability
All data associated with this study are present in the paper.

REFERENCES

1. Aamir M, Alam M, Anas SM. Effect of blast location and explosive mass on the dynamic behavior of a bowstring steel highway girder bridge subjected to air-blast. Mater Today Proc 2023; 87:20-29. doi: 10.1016/j.matpr.2022.08.275
2. ABAQUS. ABAQUS/CAE FEA program version 6.15. Concrete Damage Plasticity (CDP) model, Holmquist-Johnson-Cook (HJC) model, explicit solver, three-dimensional solid element library, default keycards and keywords. ABAQUS DS-SIMULIA User Manual, US, 2017.
3. Amer A, Attia W, Elwan S, Tamer K. Behavior of Composite Steel I-Girder Bridges under Blast Loads above Bridge Surface. Int J Civ Eng Technol 2019; 10(10):479-488.
4. Amer A, Attia W, Tamer K. Behavior of Composite Steel I-Girder Bridges Under Blast Loads Below Bridge Surface. Int J Sci Technol Res 2020; 9(08):517-522.
5. Anas SM, Alam M, Tahzeeb R. Impact response prediction of square RC slab of normal strength concrete strengthened with (1) laminates of (i) mild-steel and (ii) C-FRP, and (2) strips of C-FRP under falling-weight load. Mater Today Proc 2022; 87: 07–08. doi: 10.1016/j.matpr.2022.07.324
6. Anas SM, Alam M. Performance of simply supported concrete beams reinforced with high-strength polymer re-bars under blast-induced impulsive loading. Int J Struct Eng 2022; 12(01): 62–76.
7. Asala G, Andersson J, Ojo OA. Analysis and constitutive modelling of high strain rate deformation behaviour of wire–arc additive-manufactured ATI 718Plus superalloy. Int J Adv Manuf Technol 2019; 103(1-4):1419-1431. doi: 10.1007/s00170-019-03616-2
8. Bobbili R, Madhu V. Constitutive modeling and fracture behavior of a biomedical Ti–13Nb-13Zr alloy. Mater Sci Eng A 2017; 700:82-91. doi: 10.1016/j.msea.2017.05.113
9. Braxtan NL, Whitney R, Wang Q, Koch G. Preliminary investigation of composite steel box girder bridges in fire. Bridge Struct 2015; 11(3):105-114. doi :10.3233/BRS-150089
10. Cofer WF, Matthews DS, McLean DI. Effects of blast loading on prestressed girder bridges. Shock Vib 2012; 19(1):1-18. doi: 10.3233/SAV-2012-0612

11. ECP-201. Egyptian Code of Practice for Calculation of Loads and Forces in Structures and Buildings. National Housing and Building Research Center, Cairo, 2012.
12. Forni D, Chiaia B, Cadoni E. Strain rate behaviour in tension of S355 steel: Base for progressive collapse analysis. Eng Struct 2016; 119:164-173. doi: 10.1016/j.engstruct.2016.04.013
13. Fujikura S, Bruneau M. Experimental Investigation of Seismically Resistant Bridge Piers under Blast Loading. J Bridge Eng 2011; 16(1):63-71. doi: 10.1061/(asce)be.1943-5592.0000124
14. Grys S, Trzciński WA. Calculation of Combustion, Explosion and Detonation Characteristics of Energetic Materials. Cent Eur J Energ Mater 2010; 7(2):97-113.
15. Hafezolghorani M, Hejazi F, Vaghei R, Jaafar MSB, Karimzade K. Simplified damage plasticity model for concrete. Struct Eng Int 2017; 27(1):68-78. doi: 10.2749/101686616X1081
16. Hashemi SK, Bradford MA, Valipour HR. Dynamic response and performance of cable-stayed bridges under blast load: Effects of pylon geometry. Eng Struct 2017; 137:50-66. doi: 10.1016/j.engstruct.2017.01.032
17. Hyde DW. User's Guide for Microcomputer Program CONWEP and FUNPRO, Applications of TM 5-855-1, "Fundamentals of Protective Design for Conventional Weapons". US Army Engineer Waterways Experiment Station, 1988.
18. Krauthammer T, Assadi-Lamouki A, Shanaa HM. Analysis of impulsively loaded reinforced concrete structural elements-I. Theory. Comput Struct 1993; 48(5):851-860. doi: 10.1016/0045-7949(93)90507-A
19. Lee KM, Cho HN, Choi YM. Life-cycle cost-effective optimum design of steel bridges. J Constr Steel Res 2004; 60(11):1585-1613. doi: 10.1016/j.jcsr.2003.10.009
20. Lin J, Zong Z, Gan L, Chen Z, Li M. Damage modes and residual capacity of strand cables subjected to blast loads. J Constr Steel Res 2023; 204:107855. doi: 10.1016/j.jcsr.2023.107855
21. Lin YC, Li LT, Fu YX, Jiang YQ. Hot compressive deformation behavior of 7075 Al alloy under elevated temperature. J Mater Sci 2012; 47(3):1306-1318. doi: 10.1007/s10853-011-5904-y
22. Long Y, He Y. An anisotropic damage model for concrete structures under cyclic loading-uniaxial modeling. J Phys Conf Ser 2017; 842(1):012040. doi: 10.1088/1742-6596/842/1/012040
23. Low HY, Hao H. Reliability analysis of direct shear and flexural failure modes of RC slabs under explosive loading. Eng Struct 2002; 24(2):189-198. doi: 10.1016/S0141-0296(01)00087-6
24. Lv C, Yan Q, Li L, Li S. Field test and probabilistic vulnerability assessment of a reinforced concrete bridge pier subjected to blast loads. Eng Fail Anal 2023; 143:106802. doi: 10.1016/j.engfailanal.2022.106802
25. Maiorana E, Tetougueni C, Zampieri P. Effect of blast load on the Structural Integrity of steel arch bridge slab. Eng Fail Anal 2022; 139:106498. doi: 10.1016/j.engfailanal.2022.106498
26. Pan Y, Chan BYB, Cheung MMS. Blast Loading Effects on an RC Slab-on-Girder Bridge Superstructure Using the Multi-Euler Domain Method. J Bridge Eng 2013; 18(11):1152-1163. doi: 10.1061/(asce)be.1943-5592.0000457
27. Riedel W, Mayrhofer C, Thoma K, Stolz A. Engineering and numerical tools for explosion protection of reinforced concrete. Int J Prot Struct 2010; 1(1):85-102. doi: 10.1260/2041-4196.1.1.85
28. Stewart MG, Mueller J. Terrorism risks for bridges in a multi-hazard environment. Int J Prot Struct 2014; 5(3):275-289. doi: 10.1260/2041-4196.5.3.275
29. Tahzeeb R, Alam M, Sayed M. Performance of composite and tubular columns under close-in blast loading: A comparative numerical study. Mater Today Proc 2022; 65:51–62. doi: 10.1016/j.matpr.2022.04.587
30. TM 5-1300. Structures to resist the effects of accidental explosions. Army Technical Manual (TM 5-1300) Washington, DC. US Army, Navy Air Force, 1990.
31. Tokal-Ahmed YM. Response of bridge structures subjected to blast loads and protection techniques to mitigate the effect of blast hazards on bridges. RUcore: Rutgers University Community Repository Search Services Collections 2009.
32. Ullah A, Ahmad F, Jang HW, Kim SW, Hong JW. Review of analytical and empirical estimations for incident blast pressure. KSCE J Civ Eng 2017; 21(6):2211-2225. doi: 10.1007/s12205-016-1386-4
33. Vinitha P, Ajay VJ, Senthil-Pandian M. Comparative behavioural study of curved composite steel box and I girder using Midas. Int J Civ Eng Technol 2017; 8(4):1268-1278.
34. Winget DG, Marchand KA, Williamson EB. Analysis and Design of Critical Bridges Subjected to Blast Loads. J Struct Eng 2005; 131(8). doi: 10.1061/(asce)0733-9445(2005)131:8(1243)
35. Xiao W, Andrae M, Ruediger L, Gebbeken N. Numerical prediction of blast wall effectiveness for structural protection against air blast. Procedia Eng 2017; 199:2519-2524. doi: 10.1016/j.proeng.2017.09.432
36. Yang S, Liu Z, Wang S, Zhong W, Zhang R, Yao X. Dynamic response and failure analysis for urban bridges under far field blast loads. Eng Struct 2023; 285(1):116043. doi: 10.1016/j.engstruct.2023.116043

37. Zhou XQ, Hao H. Numerical prediction of reinforced concrete exterior wall response to blast loading. Adv Struct Eng 2008; 11(4):355-367. doi: 10.1260/136943308785836826
38. Zhu Z, Li Y, He S, Ma C. Analysis of the failure mechanism of multi-beam steel–concrete composite bridge under car explosion. Adv Struct Eng 2020; 23(3):538-548. doi: 10.1177/1369433219876185